Mon. Not. R. Astron. Soc. **000**, 1–10 (1996) Printed 20 January 1997 (MN LATEX style file v1.3)

Collimation of magnetically driven jets from accretion disks

H.C. Spruit, T. Foglizzo, and R. Stehle
Max Planck Institute for Astrophysics, Box 1523, D-85740 Garching, Germany

Accepted xx. Received xx

ABSTRACT
We argue that the toroidal fields developing in a magnetically accelerated jet are sufficiently unstable that they can not contribute much to collimation. We show how an initially collimated jet is decollimated by decay of the toroidal field and by the buildup of internal pressure due to kink instability. Instead, we propose that most of the collimation of observed jets is due to the poloidal field anchored in the disk. We show how the collimation by this mechanism depends on the distribution of poloidal field strength in the disk. We find that the maximum achievable collimation increases with the ratio of outer to inner disk radius, and can be of the order of one degree. This dependence is found to be consistent with the available data, in particular the absence of collimated outflows from Cataclysmic Variables. Because of the decay of the toroidal field a new characteristic distance plays a role, the collimation distance z_c, of the order of the disk radius or less. Beyond z_c the jet is entirely ballistic and only weakly magnetic. No external medium is needed beyond this distance to explain observed narrow opening angles of jets, and no interaction with an external medium is necessary to explain the parallel field orientation observed in fast jets.

Key words: Accretion, accretion discs – Magnetohydrodynamics – Instabilities – ISM: jets and outflows

1 INTRODUCTION

The magnetohydrodynamic model for accelerating jets enjoys popularity, among other reasons, for being the only one proposed so far that can simultaneously explain high degrees of collimation and relativistic flow speeds (for reviews see Blandford 1993, Königl and Ruden 1993; for an introduction see Spruit, 1996). In this model, there is a magnetic field in the accretion disk which accelerates a flow centrifugally in an 'inner' region, in which the field energy density is large compared with the energy density in the flow. The boundary of this region is the Alfvén surface, typically at a rather large distance from the point on the disk where the flow was launched. Outside this is an outer region where the flow speed exceeds the Alfvén speed and the flow stops being accelerated. In this region, the flow also stops corotating with the disk, so that a loop of toroidal (azimuthal) field is added to the flow for each rotation of the foot point of the field line. As a result, in axisymmetric models, a highly wound up nearly toroidal field develops beyond the Alfvén surface. The tension of this wound-up field ('hoop stress') produces a force directed towards the axis. In most models of magnetic acceleration developed so far, the collimation of the jet is due to this effect. Heyvaerts and Norman (1989, see also Heyvaerts and Norman 1997) using methods of asymptotic expansion, showed that depending on conditions at the base of the flow, the jet at large distance has either a cylindrical, a parabolic or a conical shape. Li et al. (1992) showed how the formation of weakly collimated, conical flows depends on the shape of the poloidal⋆ field near the Alfvén surface. The transition between such weakly collimated flows and highly collimated jets was studied by Sauty and Tsinganos (1994).These studies were done for the nonrelativistic case. For work on the collimation properties of relativistic flows see Appl and Camenzind (1993), Nitta (1994), Tomimatsu (1994) and Fendt et al. (1995).

Axisymmetric models are attractive because they are numerically tractable and their relative simplicity allows many details of the flow to be calculated accurately. The neglect of nonaxisymmetric processes, however, gives a distorted view of the physics. In particular, the highly wound up fields beyond the Alfvén surface are unlikely to be realistic. From experience in other contexts, such fields are known to be violently unstable to nonaxisymmetric insta-

⋆ The labels poloidal and toroidal are reversed here with respect to the convention for cylindrical configurations in the plasma literature. This is because the jets we consider have their axis along the symmetry axis rather than the azimuthal direction.

bilities (kink instability). These instabilities play a major role in the design of plasma confinement devices (e.g. Bateman, 1980). In stellar interiors toroidal fields are unstable for all field strengths, even if a strongly stabilizing stratification is taken into account (Tayler 1980, Pitts and Tayler 1985). These instabilities derive their energy from the free energy B_ϕ^2 in the toroidal field. To the extent that collimation is actually due to the toroidal field, instability therefore directly affects jet collimation, as argued before by Eichler (1993). The instability converts energy in the toroidal field to other forms of energy: a nonaxisymmetric field component, kinetic energy, and heat or fast particles. These other forms do not disappear immediately, but stay in the system for a while and add to the internal pressure of the jet. Indirectly, through the outward force resulting from the enhanced internal pressure, instability therefore has an additional decollimating effect.

We conclude that the issue of instability must be faced in the context of jet collimation. Linear stability calculations in the context of jets have been done by Appl (1996), Appl and Camenzind (1992) and others. The effects on collimation, however, require a study of the nonlinear development. Since the instability destroys not only the axisymmetry but also the stationarity of the flow, a full study of its effects requires 3-dimensional time dependent MHD simulations. Such simulations have been done by Todo et al. (1993) and Lucek and Bell (1996). These results confirm the strong tendency to develop kink instability. Lucek and Bell stress, in particular, the damaging effect this has on collimation of the flow. If these results are representative, one would conclude that collimation by hoop stresses is not possible.

In observed jets, the range of length scales over which collimation is observed is very large, often exceeding a factor 10^6 ($<$ 0.1 pc VLBI scale to $>$ 100kpc scale in AGN jets, for example). A jet which is decollimated by some instability in its inner regions may conceivably be recollimated again at a larger length scale. This possibility suggests itself in particular for magnetically collimated jets, because on expansion of the jet (perpendicular to its axis) the azimuthal field component decreases less rapidly than the axial component. Unless the azimuthal component is continually destroyed, it will eventually become larger than the axial component again, and the possibility of re-collimation (on a much larger length scale) must be adressed. This tendency towards recollimation by the azimuthal field is central also in the theorems that have been developed (Sakurai 1985, Heyvaerts and Norman, 1989) about the asymptotic collimation of axisymmetric magnetic jets. Sakurai, for example, shows that an initially purely radial stellar wind in an initially radial field ultimately can be collimated competely towards the rotation axis, even though the hoop stress decreases monotonically along all flow lines (see also Li, 1996). The process, however, takes several decades in radius.

Three-dimensional numerical simulations covering the large range in length scales required to follow the jet's collimation history from the Alfven surface up to oberved length scales can not be done at present. The effects can already be demonstrated by more simplified calculations, however. This is done in the first part of this paper. The conclusion will be that instability is indeed likely to lead to serious decollimation. The tendency for the azimuthal field to increase relative to the poloidal component plays some role when a large range in length scales is considered, but can not effectively prevent decollimation by the instability.

An alternative collimation mechanism is therefore called for. In section 4, we show that the magnetic field carried by the disk can be a powerful collimator ('poloidal collimation'), under modest assumptions about its strength and distribution in the disk. In this mechanism (proposed before by Blandford 1993, Spruit 1994), the degree of collimation that can be achieved is related to the ratio of outer to inner disk radius, which has to be sufficiently large. In the last section we discuss the observational evidence in this context and find that, in particular, the absence of collimated outflows from Cataclysmic Variables is nicely understood in this picture.

Numerical results in which collimation by the poloidal field component anchored in the disk plays a role have been available for some time (Uchida and Shibata 1984, 1985, Sauty and Tsinganos 1994, Bell and Lucek 1995). The field of a magnetized disk looks like a dipole, at large distances, and therefore does not have any collimating virtues at such distances. The question of collimation behavior over a large range in length scales therefore arises in this context as well, and is adressed with the model developed in sections 3 and 4.

2 KINK INSTABILITY

For a discussion of instabilities it is sufficient, to first approximation, to assume the jet to be cylindrical and nearly perfectly collimated. While less collimated outflows are also of interest, the strongest observational constraints on (de)collimation processes come from the most collimated jets (protostellar and extragalactic type II jets), for which a nearly cylindrical geometry is a good approximation. By moving into a frame comoving with the mean motion of the jet, the stability problem reduces to a nearly static one, as long as interaction of the jet with its surroundings is small. Models in which the collimation is related to hydrodynamic interaction of the jet with its surroundings abound in the literature (see Peter and Eichler 1993, 1995 and references therein), but we may neglect such interaction at this point since the process of collimation by hoop stresses does not depend on it.

The stability of a static, twisted cylindrical field configuration has been studied at great length in the controlled fusion contex (e.g. Bateman, 1980). The most damaging instabilities are ideal-MHD instabilities, which do not depend on diffusive processes and take place on a dynamical time scale. We concentrate here on ideal MHD instability, and ignore diffusion-related instabilities like tearing modes.

In the absence of external stabilizing surfaces, cylindically symmetric configurations are typically unstable to an $m = 1$ kink mode for any degree of twist. Stability can be achieved by limiting the motion of the plasma by enclosing it in an outer cylinder, or between two surfaces perpendicular to the axis. In the latter case, one finds that instability typically sets in when the field lines make more than one turn around the axis between the two surfaces (Kruskal-Shafranov condition). The stability problem is a global one. A magnetic surface in the configuration which is unstable by this condition can be stabilized in principle by surrounding stable magnetic volumes. However, when a systematic twist is present in the configuration, the Kruskal-Shafranov condition is a good approximation for the onset of instability. Such a systematic twist is present in the magnetically collimated jet. Stabilizing surfaces along or perpendicular to its axis are absent. To the extent that the jet can be approximated by a cylindrical equilibrium without external surfaces, it is therefore bound to be unstable.

Whether the instability does any significant damage to the collimation of the jet is a second question; this depends on the growth rate and on the nature of the final state it reaches. The free energy on which the instability feeds is B_ϕ^2, the energy in the toroidal field component. If r is the jet radius, the growth rate of the instability is of the order $\eta = B_\phi/(4\pi\rho r^2)^{1/2}$, where ρ is the density (Bateman, section 6.4). In order for the hoop stress to have a significant collimating effect, B_ϕ must be at least as large as the axial component B_z. Thus, the instability grows fastest for the narrowest jets (at given B_z and ρ). The conditions under which the growth is fast enough to affect collimation are discussed in the next section. Details of the nonlinear development of the instability are available from numerical simulations, such as those by Horiuchi and Sato (1986), Craig and Sneyd (1990), Todo (1993) and Galsgaard (1996). These simulations show a rapid initial development on the time scale predicted from linear theory. After this, the configuration evolves more slowly.

An important role is played by the *magnetic helicity* $H = \int \mathbf{B}\cdot\mathbf{A}$ (where $\mathbf{A}$ is the vector potential) a global quantity of the configuration (Woltjer, 1958) which is constant in time as long as diffusion and reconnection can be ignored. It is a measure of the degree of twist in the field configuration. By Taylor's (1974) assumption, this quantity is still approximately constant, for example during kink instability, even when diffusion is present. This is borne out by numerical simulations of unstable sheared configurations (Horiuchi and Sato 1986, Galsgaard 1996), which show that the helicity decays on a long time scale compared with the dynamical time scale. Königl and Choudhuri (1985), Choudhuri and Königl (1986, see also Villata and Ferrari 1994) have constructed helical MHD equilibria and applied them to jets, the point of view being that kink instabilities might lead to new equilibrium states. Instead, we base our considerations here on the results from the time dependent simulations mentioned, which indicate a much more drastic evolution of kink instability.

The instability decreases the twisting of the axisymmetric part of the field, by creating a nonaxisymmetric component which in a somewhat loose sense 'carries the excess twist'. A way of visualizing this is by analogy with a twisted rubber band under tension; beyond a certain number of twists, the band kinks. The net number of turns in the system does not change ('helicity conserved'), but one turn of twist around the axis is exchanged for one 'geometrical' turn due the looping path of the axis. As in the magnetic case, stress energy due to twisting is relieved at the expense of stretching the band somewhat (which requires work to be done against the tension). As in the case of the rubber band, the nonaxisymmetric component occupies additional volume. If the system is confined to a fixed volume, it increases the magnetic pressure.

As applied to the collimation of jets, this implies that the instability has two separate decollimating effects. First, it reduces the hoop stress by reducing the strength of the mean toroidal field; secondly the kinks add a field component which increases the internal pressure. Both effects take place on the time scale of the instability, the dynamical time scale given by the time for an Alfvén wave to cross the jet radius. The internal pressure generated decays again, but this takes place on the longer time scale related to the dissipation of magnetic helicity.

3 EFFECT OF KINK INSTABILITY ON COLLIMATION

We illustrate here the destructive effect of kink instability on the collimation of jets with a one-dimensional model. We assume that the flow speed along the jet is constant, and that the jet expands slowly with distance (i.e. the collimation is good). The expansion of the jet is represented by a single function $r(z)$, the jet radius as a function of distance.

Because of our assumption of slow expansion, the evolution of the jet is conveniently described in a frame comoving with the axial flow. In this frame, the jet radius is a slowly evolving function of time, and the task is to find appropriate equations for this time dependence. Since the instability is dynamical and driven by the energy in the toroidal component of the field, kink instability takes place with a growth rate $v_{\mathrm{A}\phi}/r$, where $v_{\mathrm{A}\phi}$ is the Alfvén speed based on the toroidal field component, $v_{\mathrm{A}\phi} = B_\phi/(4\pi\rho)^{1/2}$.

The 'hoop stress' due to this field component disappears at this same time scale. If the instability were to take place in an initially static situation, the field configuration would expand on this time scale, and then evolve more slowly because of approximate helicity conservation. In our case, the background is expanding. Any azimuthal field left after the kink instability now increases relative to the axial field because of expansion. The field is then again unstable to kinking, though on a longer time scale. Some form of kink must therefore operate more or less continuously in an expanding jet. The rate at which this happens is the Alfvén rate, hence $\mathrm{d}\ln(B_\phi)/\mathrm{d}t \approx -v_{\mathrm{A}\phi}/r$, and our first estimate of the time dependence of B_ϕ is

$$\frac{\mathrm{d}B_\phi}{\mathrm{d}t} = -\gamma\frac{B_\phi}{(4\pi\rho)^{1/2}r}B_\phi,$$

where γ is a factor of order unity.

This equation requires some modification, since the instability takes place in a slowly expanding environment. In a homologously expanding axisymmetric jet, in the absence of nonaxisymmetric instabilities, one finds (from the MHD induction equation) that the toroidal and poloidal field components depend on the expansion factor r/r_0 as

$$B_\phi = B_{\phi 0}(r/r_0)^{-1}, \qquad B_z = B_{z0}(r/r_0)^{-2}. \tag{1}$$

Thus, the quantity rB_ϕ changes by instability, but not by expansion alone, and a slow expansion is taken into account approximately by writing

$$\frac{1}{r}\frac{\mathrm{d}}{\mathrm{d}t}(rB_\phi) = -\gamma\frac{B_\phi^2}{(4\pi\rho)^{1/2}r}. \tag{2}$$

The energy liberated by the instability does not disappear in place, but is converted into fast particles, heat, kinetic energy, and a nonaxisymmetric field component. Each of these increases the effective pressure in the jet. A part of this energy, namely the fraction that goes into fast particles, may disappear on a short time scale by radiation, but much of the energy stays in the system. The nonaxisymmetric field component, for example, decays on a much longer time scale than the instability time scale, in connection with the approximate conservation of magnetic helicity discussed above. Let $P_{\rm i}$ be the internal pressure in the system resulting from the energy liberated by the instability. Ignoring the expansion of the jet for the moment, $P_{\rm i}$ changes as

$$\frac{\mathrm{d}P_{\rm i}}{\mathrm{d}t} = -f\frac{\mathrm{d}}{\mathrm{d}t}(B_\phi^2/8\pi),$$

where f is the fraction of the energy which stays in the system. As the jet expands, $P_{\rm i}$ diminishes by adiabatic expansion. To take this into account, we have to associate a compressibility to $P_{\rm i}$. For simplicity, we assume that $P_{\rm i}$ varies like the pressure of a magnetic field expanding perpendicular to the field lines (the results are not very sensitive to this, as the effect of $P_{\rm i}$ will turn out to be only modest). On expansion, $P_{\rm i}$ then varies as $P_{\rm i} \sim r^{-4}$. Taking this into account the equation for $P_{\rm i}$ becomes

$$\frac{1}{r^4}\frac{\mathrm{d}}{\mathrm{d}t}(r^4 P_{\rm i}) = -f\frac{B_\phi}{4\pi}\frac{\mathrm{d}B_\phi}{\mathrm{d}t}. \tag{3}$$

Finally, the equation of motion perpendicular to the jet axis determines the actual rate of expansion $r(t)$. If $v_\perp$ is the perpendicular velocity, we have, ignoring gas pressure but including the instability-generated pressure $P_{\rm i}$:

$$\rho\frac{\mathrm{d}v_\perp}{\mathrm{d}t} = -\partial_r\left(\frac{B_\phi^2+B_z^2}{8\pi}+P_{\rm i}\right) - \frac{B_\phi^2}{4\pi r}. \tag{4}$$

If we now approximate to one dimension by writing $\partial_r = -1/r$ and $v_\perp = \mathrm{d}r/\mathrm{d}t$, we get as our equation of motion

$$r\rho\frac{\mathrm{d}^2 r}{\mathrm{d}t^2} = (B_z^2 - B_\phi^2)/8\pi + P_{\rm i}. \tag{5}$$

This equation can be derived a bit more formally by considering a model system consisting of a cylinder of radius r with a uniform density and poloidal field, surrounded by a purely toroidal vacuum field. For uniform expansions and contractions of this cylinder, one then finds eq. (5). The density ρ varies as r^{-2}. Let r_0, ρ_0 be the jet radius and density at $t=0$, $B_{\phi 0}$ and B_{z0} the axisymmetric field components at that time. Let

$$t_0 = r_0(8\pi\rho_0)^{1/2}/B_{\phi 0}, \qquad \alpha = B_{z0}/B_{\phi 0}, \tag{6}$$

$$\tau = t/t_0, \qquad x = r/r_0, \qquad b = B_\phi/B_{\phi 0}, \tag{7}$$

$$p = 8\pi P_{\rm i}/B_{\phi 0}^2, \tag{8}$$

then equations (2), (3), (5) can be written as

$$\frac{\mathrm{d}^2 x}{\mathrm{d}\tau^2} = x(\frac{\alpha^2}{x^4} + p - b^2), \tag{9}$$

$$\frac{1}{x^4}\frac{\mathrm{d}}{\mathrm{d}\tau}(x^4 p) = 2\gamma f b^3, \tag{10}$$

$$\frac{1}{x}\frac{\mathrm{d}}{\mathrm{d}\tau}(xb) = -\gamma x b^2. \tag{11}$$

The initial conditions at $t=0$ are $b(0)=1$, $x(0)=1$, $p(0)=0$, and a value for the initial expansion rate $\mathrm{d}x/\mathrm{d}\tau$ which is related to the initial opening angle $\theta_0 = (v_\perp/v_\parallel)_0$.

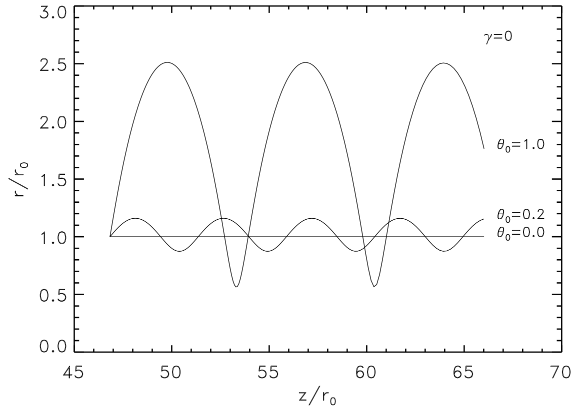

Figure 1. Collimation of a jet by 'hoop stress' due to the toroidal field, in the absence of kink instability. Parameter is the initial collimation angle θ_0. The oscillation is a compressional mode excited when the initial collimation angle does not match the final collimation.

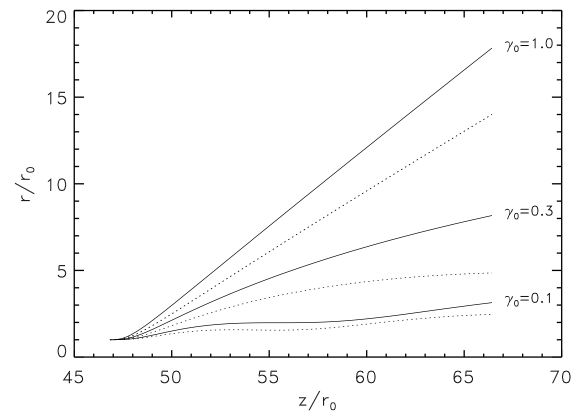

Figure 2. Decollimation of the jet due instability of the toroidal field. Jet is assumed to be perfectly collimated at the start ($\theta_0 = 0$). Solid lines: including internal pressure generated by the instability ($f=1$), dashed: without ($f=0$). Parameter γ is the assumed growth rate of the instability in units of the nominal rate $v_{\rm A}/r$.

As starting point of the calculation we take a point near the Alfvén surface, where $v_\parallel$ and $v_{\rm A0}$ are of the same order. To make this more specific, we take the starting point at the location where $v_\parallel\sqrt{2} = v_{\rm A}$. With this choice we have

$$\theta_0 = \frac{1}{v_\parallel}(\mathrm{d}r/\mathrm{d}t)_0 = \frac{v_{{\rm A}\phi 0}}{v_\parallel\sqrt{2}}(\mathrm{d}x/\mathrm{d}\tau)_0 = (\mathrm{d}x/\mathrm{d}\tau)_0. \tag{12}$$

The initial opening angle θ_0 is varied as a parameter of the problem. The distance traveled by the jet is related to τ by

$$z = r_0\tau. \tag{13}$$

Finally, we assume that the initial acceleration vanishes, in order to get a 'soft' start. This requires $\alpha = 1$, which is consistent with the fact that the toroidal and poloidal field components are of comparable magnitude at the Alfvén surface, in the magnetic acceleration model. Solutions of eqs. (9)-(11) are shown in figures 1, 2. Figure 1 shows the response of the jet to different initial conditions, in the absence of instability ($\gamma = 0$). The jet stays perfectly collimated, $\mathrm{d}r/\mathrm{d}z = 0$, if it is initially collimated ($\theta_0 = 0$). If the initial collimation is not perfect, an oscillation takes place whose amplitude depends on the initial conditions. This is a compressional mode of the jet. In the compressed phase, the outward pressure due to the axial field dominates, in the expanded phase the inward hoop stress of the azimuthal field dominates. Oscillations of this kind are also seen in two-dimensional jet calculations, e.g. Sauty and Tsinganos (1994, their figure 8).

Figure 2 shows the effect of the instability on collimation. If the growth rate of the instability is taken equal to its nominal value, the dynamical time scale $v_{\rm A}/r$ (i.e. if $\gamma = 1$), an initially perfectly collimated jet decollimates completely into a flow with opening angle of order 45°. Part of the decollimation is due to the internal pressure generated by the instability, but even if this contribution is ignored ($f = 0$, dashed lines), the decollimation is essentially complete. The effect can be reduced only by arbitrarily assuming that the growth rate is significantly *less* than the dynamical time scale, by setting $\gamma < 1$. If this is done, the final collimation angle is roughly proportional to γ:

$$\theta_\infty \approx \gamma. \tag{14}$$

We conclude that high degrees of jet collimation by hoop stresses are impossible in the presence of any significant level of kink instability.

4 POLOIDAL COLLIMATION

The magnetic field carried by the disk can either be internally generated by some dynamo process, or it could consist of poloidal field lines captured from the environment that supplied the mass for the disk. In either case, the field is likely to increase in strength toward the center of the disk. If the field is dynamo-generated, its energy density is likely to saturate at some fraction of the gas pressure (as shown be recent simulations by Brandenburg et al. 1995, Hawley et al. 1995). Captured fields increase in strength toward the center due to compression by the accretion flow. At the same time however, the amount of *magnetic flux* in these central regions may well be small compared with the total poloidal flux in the disk, simply for geometrical reasons. Assume now that this is the case, and that the vertical field component at the disk surface is a smooth function of radius. As an example, take

$$B_z \sim (r^2/r_{\rm i}^2 + 1)^{-\mu/2}, \tag{15}$$

where $r_{\rm i}$ is the radius of the inner edge of the disk. If $\mu > 0$, the field strength increases towards the center. If $\mu < 2$, the magnetic flux crossing the disk, $\Phi \sim r^{2-\mu}$ increases with r. The self similar model of Blandford and Payne (1982), for example, corresponds to $\mu = 5/4$. If the Alfvén surface is at sufficient distance from the disk surface, the field near the disk is approximately a potential field, $|\nabla \times \mathbf{B}| \ll B/r$. Such a field is uniquely determined by the distribution of flux at the disk surface, $B_z(r, z = 0)$, which acts as boundary condition for the potential problem. An example is shown in figure 3, which is the solution of this potential problem with (15) as boundary condition, and with $\mu = 1$ (Cao and Spruit 1994). Along the disk surface, the field lines fan out away from the axis, due to the high field strength in the center. In the vertical direction, however, the field bends toward the

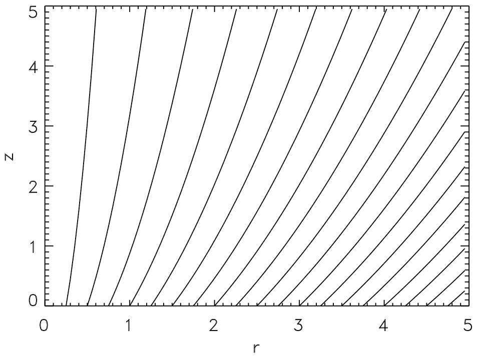

Figure 3. Field lines of a potential field above an accretion disk, produced by a distribution of surface field strength according to eq. 15 with $\mu = 1$

axis. This is due to the fact that most of the magnetic flux is in the outer parts of the disk. With increasing distance above the disk, the potential becomes more and more influenced by these outer field lines (see also figure A1 in Sakurai, 1987). By the nature of potentials, the field strength at a distance z above the disk is of the order $B(r = z, z = 0)$. The shape $R(z)$ of a field line close to the axis is given approximately by $R^2 B_z =$ cst., or $R \sim z^{\mu/2}$. This implies $\mathrm{d}R/\mathrm{d}z \to 0$ for $z \to \infty$ i.e. the field lines have a 'collimating' shape as long as $\mu < 2$.

If a magnetic wind is launched from a disk with a field configuration like figure 3, the field is distorted by the flow, but these distortions remain small until the Alfvén radius is reached. The flow is then already highly collimated, by the poloidal field of the disk. Even if no further collimation takes place beyond the Alfvén surface, neither by the poloidal nor the toroidal field, a collimated jet can result. The collimation is best, in this scheme, if the Alfvén surface is at a large height above the disk because the bending of the field lines toward the axis takes place gradually.

4.1 The collimation distance

In the example above the collimation angle can be made arbitrarily small, by taking the Alfvén surface far enough from the disk, because the disk was assumed to be infinite in size. The potential field produced by a disk of finite size, when seen from a sufficient distance, is a dipole, whose field lines have a decidedly *decollimating* shape (all field lines from the center return back to the midplane). Poloidal collimation by disks of finite size therefore works best if the Alfvén surface is neither to close to the disk surface, nor too far away. In this section we show how much collimation one can expect to achieve by disks of finite size.

Figure 4 shows an example of a field configuration from a finite disk. Instead of specifying $B_z(r)$ on the disk surface, this field was constructed by specifying the azimuthal current density $j(r)$ on the disk surface (which is technically easier). The current distribution is given by

$$j = (r^2 + 1)^{-1/2} \quad (r < 1), \qquad j = 0 \quad (r > 1). \tag{16}$$

The vertical field component $B_z(r)$ at the disk surface produced by this current is close to the form (15) with $\mu = 1$, except near the disk edge at $r = 1$. In the inner regions, the

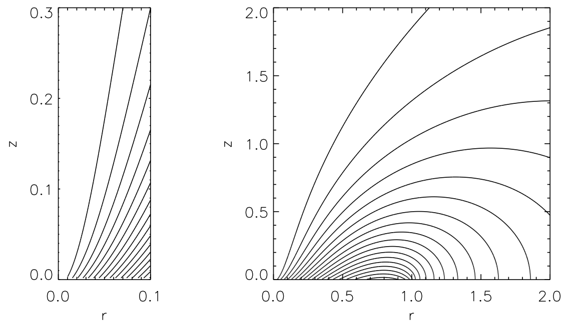

Figure 4. Field line shapes of a potential field produced by a disk of finite size ($r=1$), in which the field strength is maximal at disk center, but most of the magetic flux resides in the outer parts of the disk. On a large scale the field resembles that of a dipole (right panel), but in the inner regions (left) it has a highly collimating shape.

field is therefore close to that of figure 3 The numerical procedure used for computing this field configuration is given elsewhere (Stehle, 1997).

The collimation by a field like figure 4 can be estimated as follows (a more accurate numerical result is presented in section 4.3). As long as the external field is strong enough we can assume equilibrium between the internal pressure of the jet and the external magnetic pressure. Ignoring the toroidal field as well as the internal pressure it creates, this means that the internal poloidal field strength $B_{\rm i}$ equals the external field $B_{\rm e}$. If the jet is narrow, its effect on the surrounding field configuration is small. The external field lines are pushed aside a bit, but their field strength is nearly unchanged. The equilibrium condition is then

$$B_{{\rm i}z}(z)=B_{{\rm e}z}(r=0,z), \tag{17}$$

where $B_{\rm e}$ is a known function of the field distribution on the disk surface. The internal field scales with the jet radius r as r^{-2}, so

$$(r/r_0)^2=B_{\rm e0}/B_{\rm e}(0,z), \tag{18}$$

where $B_{\rm e0}=B_{\rm e}(0,z_0)$ is the external field at the height z_0 where we start the jet calculation (the Alfvén surface) and r_0 the jet radius at that point. Assuming the flow speed along the jet to be constant, the density in the jet varies as

$$\rho/\rho_0=(r/r_0)^{-2}, \tag{19}$$

so that the Alfvén speed in the jet varies as

$$\frac{v_{\rm A}}{v_{\rm A0}}=\frac{B_{\rm e}(z)}{B_0}\frac{r}{r_0}=(B_{\rm e}(z)/B_0)^{1/2}. \tag{20}$$

The Alfvén speed therefore decreases with distance, and there comes a point where the radial expansion speed $v_\perp = {\rm d}r/{\rm d}t$ becomes comparable to $v_{\rm A}$. Beyond this point, equilibrium between the internal and external pressure is no longer satisfied, since information required to establish equilibrium can propagate across the jet only at the Alfvén speed (in the form of a fast mode wave). Let the distance along the axis where this happens be called the *collimation distance* $z_{\rm c}$. At $z_{\rm c}$ the collimating effect of the external field stops, and the radial expansion speed does not change any more after $z_{\rm c}$. The jet now expands ballistically at constant opening angle $\theta_\infty = v_\perp/v_\parallel$. This asymptotic collimation angle depends on the height of the Alfvén surface, the particulars of the field distribution on the disk, and on the size of the disk. We first give some analytical estimates of these dependences, followed by numerical results using the model of section 3.

4.2 Analytical estimates

An estimate of the asymptotic opening angle of the jet is obtained by assuming that the flow follows the poloidal field lines exactly up to the distance of last collimation $z_{\rm c}$, and at that point instantly ‘detaches’ from the field. The collimation angle θ then equals the angle of the poloidal field line with respect to the axis at $z_{\rm c}$. This angle depends on the shape of the poloidal field lines. We compute it for finite disk of radius R with a distribution of current $j(r)$ given by:

$$j(r)=J_0\left(\frac{R}{r}\right)^\mu \quad (0<r<R), \qquad j(r)=0 \quad (r>R), \tag{21}$$

where $\mu \in]0,2[$. This current density, and the resulting field configuration are singular at the origin, and only there. In particular the field is regular on the axis.

Since we are interested in well collimated jets, we can limit attention to field lines near the axis. We derive in the Appendix the first order expansion of the magnetic field $\mathbf{B}$ created by (21), for $r \ll R$ and $r \ll z$:

$$B_r = \frac{\pi J_0}{K_1}\frac{r}{z}\left(\frac{R}{z}\right)^\mu\left\{1+3K_1\int_0^{\frac{z}{R}}\frac{u^{\mu+1}{\rm du}}{({\rm u}^2+1)^{\frac{5}{2}}}\right\} \tag{22}$$

$$+\mathcal{O}\left(\frac{r^3}{R^3}+\frac{r^3}{z^3}\right), \tag{23}$$

$$B_z = \frac{2\pi J_0}{\mu K_1}\left(\frac{R}{z}\right)^\mu\left\{1-\mu K_1\int_0^{\frac{z}{R}}\frac{u^{\mu+1}{\rm du}}{({\rm u}^2+1)^{\frac{3}{2}}}\right\} \tag{24}$$

$$+\mathcal{O}\left(\frac{r^3}{R^3}+\frac{r^3}{z^3}\right), \tag{25}$$

where the factor $K_1(\mu)$ is defined in the Appendix.

The direction of the field lines is measured by their angle $\theta(r,z)$ with the axis of symmetry:

$$\tan\theta \equiv \frac{B_r}{B_z}. \tag{26}$$

By taking the limit $r \ll z \ll R$, we obtain

$$\mathbf{B}\cdot\nabla\tan\theta \sim -\frac{rB_z}{z^2}\frac{\mu(2-\mu)}{4}<0. \tag{27}$$

This proves that near the surface of the disk, the angle θ decreases upwards along a field line. This angle ultimately increases since all field lines cross the equatorial plane outside the disk. The height $z_{\rm x}$ where the angle is minimum, for field lines close to the axis, is the solution of an integral equation derived in the Appendix, which we solve numerically. As shown in Fig. 5, the inflection point is located roughly at $z_{\rm x}=0.2R$ for most values of μ, with a significant decrease when μ is close to 2.

The minimum angle $\theta_{\rm min}$ depends on the distance $r_{\rm i}$ of the foot point of the field line from the axis. For $r_{\rm i} \ll R$, we obtain:

$$\theta_{\rm min} \sim C\left(\frac{r_{\rm i}}{R}\right)^{1-\frac{\mu}{2}}\left[1-K_2\left(\frac{r_{\rm i}}{R}\right)^\mu\right]^{\frac{1}{2}}, \tag{28}$$

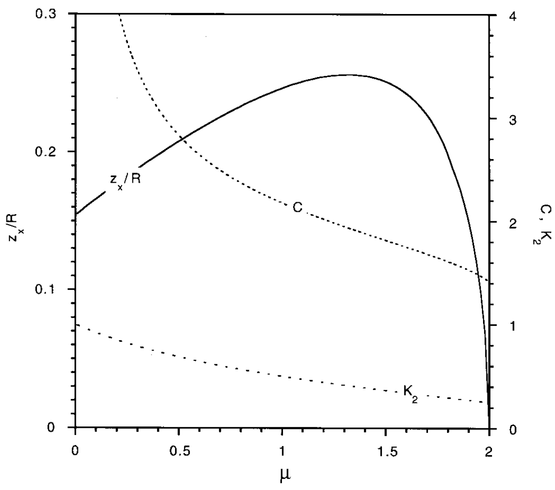

Figure 5. Height z_{x} above the disk of the inflection point in the field line shape (solid) and the coefficients C and K_2 determining it, cf. Equation (28)

The factors C and K_2 depend on μ only; they are derived in the Appendix and displayed in Fig. 5 together with z_{x}. The term containing K_2 is important only in the limit $\mu \to 0$, and can be neglected otherwise. Although C diverges for $\mu \to 0$, the quantity $C(1-K_2)^{1/2}$ is of order unity, indicating that the minimum angle scales like

$$\theta_{\min} \approx \left(\frac{r_{\mathrm{i}}}{R}\right) \log\left(\frac{R}{r_{\mathrm{i}}}\right) \qquad (\mu \to 0). \tag{29}$$

For $\mu = 1$, for example, we get from (28) and figure (5):

$$\theta_{\min} \approx 0.2 \left(\frac{r_{\mathrm{i}}}{R}\right)^{\frac{1}{2}}, \quad (\mu = 1) \tag{30}$$

in agreement with the estimate given earlier in Spruit (1994).

These estimates do not take into account the presence of the initial toroidal field. Also the radial balance of the jet is not instantaneous as assumed here, but is the result of an adjustment process that takes place on a finite time scale. These factors are taken into account in the numerical calculations of the next section.

4.3 Numerical model

We can improve on the previous estimates by adapting the model used in section 3. The only change needed to take into account the collimating effect of the disk field is to add the corresponding magnetic pressure term on the right hand side of equation (5):

$$r\rho \frac{\mathrm{d}^2 r}{\mathrm{d}t^2} = (B_z^2 - B_\phi^2 - B_{\mathrm{e}}^2)/8\pi + P_{\mathrm{i}}. \tag{31}$$

Writing

$$b_{\mathrm{e}} = B_{\mathrm{e}}/B_{\mathrm{e}0}, \qquad \beta = B_{\mathrm{e}0}/B_{\phi 0} \tag{32}$$

equation (9) becomes

$$\frac{\mathrm{d}^2 x}{\mathrm{d}\tau^2} = x\left(\frac{\alpha^2}{x^4} + p - b^2 - \beta^2 b_{\mathrm{e}}^2\right). \tag{33}$$

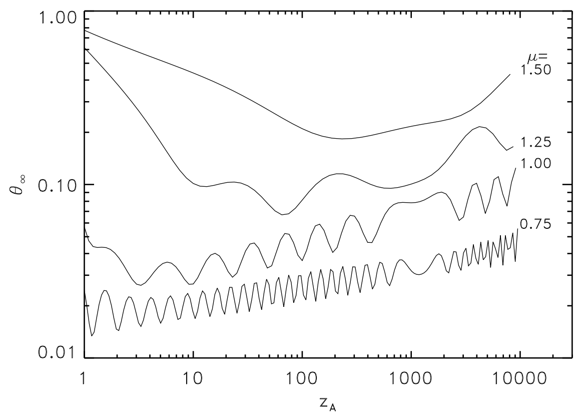

Figure 6. Asymptotic collimation angle (radians) as a function of the Alfvén distance z_{A}. Ratio of outer to inner disk radius is 10^4. Parameter is μ, the index of the radial dependence of field strength in the disk.

We take the same initial conditions as in section 3. Also, we assume again that the radial acceleration vanishes at the start of the calculation, which now implies that

$$\beta = (\alpha^2 - 1)^{1/2}. \tag{34}$$

The computations were done for the case $\alpha = 1.2$ (the results do not depend very strongly on α). For the dependence of the disk field B_{e} on height z along the axis, we take Sakurai's field configuration as described in the previous subsection, modified to take into account a finite disk size. The shape of a field line near the axis is given by

$$(r/r_{\mathrm{i}})^2 = A(z/r_{\mathrm{i}})^{-\mu} S(z/R) \qquad (0 < \mu < 2), \tag{35}$$

where

$$A = \frac{2}{(2-\mu)\Gamma(\mu)} \frac{\Gamma(\mu/2)}{\Gamma(1-\mu/2)}, \tag{36}$$

and r_{i} is the radius of the foot point of the field line on the disk. We identify r_{i} with the radius of inner edge of the disk. R is the disk radius and S takes into account the effect of a finite disk size,

$$S(\zeta) = 1 - (1 + \zeta^{\mu-3})^{-1/2}. \tag{37}$$

One verifies that this makes the field vary in dipolar fashion at large distance, $B_{\mathrm{e}} \sim z^{-3}$. At intermediate distances, (37) does not agree exactly with the analytic model of the previous subsection, but it can be regarded as a convenient analytic approximation, and is close enough for the present purpose.

Figure 6 shows the variation of the asymptotic collimation angle θ_∞ with the distance z_{A} of the Alfvén surface, for a disk radius $R/r_{\mathrm{i}} = 10^4$. The dependence is quite 'wiggly'. This is related to the radial jet oscillations discussed above (figure 1). These oscillations are a by-product of the initial conditions and the decay of the toroidal field. The asymptotic collimation angle is wider if the oscillation happens to be in an expanding phase at the moment the jet reaches the collimation distance, and narrower if it is in a contracting phase. In effect, the presence of oscillations produces a certain amount of 'deterministic noise' on the collimation angle.

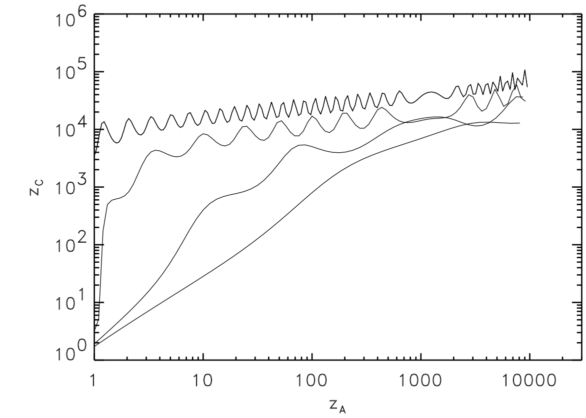

Figure 7. Dependence of the distance of last collimation z_c on the Alfvén distance $z_{\rm A}$. Values of μ are, from top to bottom: 0.75, 1.0, 1.25, 1.5.

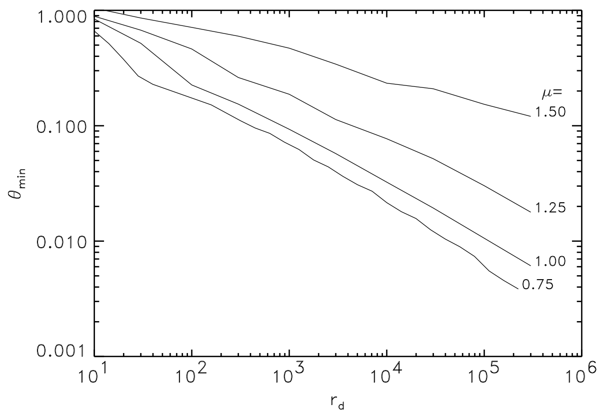

Figure 8. Optimal collimation (minima of curves in fig. 6) as a function of outer disk radius. μ is the index of the radial dependence of the field strength.

The collimation distance z_c for the same parameters is shown in figure 7. In agreement with the analytical estimate of section 4.2, the asymptotic collimation angle does not depend much on the height of the Alfvén surface (the level where the jet is launched in our calculations), if the poloidal field strength in the disk varies as r^{-1} or weaker. But even for μ as large as 1.5 the dependence on $z_{\rm A}$ is quite modest, a factor of 3 from $z_{\rm A} = 10$ to $z_{\rm A} = 10^4$. The main factors determining the collimation are the ratio of outer to inner disk radii, and the slope μ of the field strength distribution in the disk. This dependence is summarized in figure 8. It shows the minimum of the collimation angle with respect to $z_{\rm A}$, after averaging the curves of figure 6 somewhat to remove the effect of the oscillation-induced wiggles.

We conclude from these figures that very high degrees of collimation are achieved by the poloidal collimation mechanism, especially for disks with a large ratio of outer to inner radii.

4.4 Internal dynamics beyond the collimation distance

As shown by the numerical simulations of kink instability mentioned before, the disorganized field which is produced from the toroidal field decays more slowly than the ordered toroidal field itself. It is therefore likely that some of this disorganized field will survive in the flow beyond the Alfvén surface. This field component initially has an energy density of the same order as the poloidal field (since it derives from a toroidal field which was of similar strength as the poloidal field). Now the axial flow speed is likely to be somewhat nonuniform across the jet, thereby stretching the irregularities into a field which is parallel to the axis, but of fluctuating polarity. The flow rapidly becomes superalfvénic outside the Alfvén surface, so that even the *differential* flow speed can easily be superalfvénic, and stretching of the irregulaties can be quite effective. This way, the parallel field orientation seen in fast AGN jets is a natural consequence of the instability of the toroidal field. This parallel orientation has usually been attributed to an interaction of the jet with its surroundings. Stretching of internally generated irregularities will work equally well, and better in cases where the external medium is tenuous.

5 DISCUSSION

On the basis of known results from laboratory plasmas and numerical simulations, we have argued that the toroidal field traditionally held responsible for collimating jets in the magnetic acceleration mechanism is unstable on a short time scale and hence ineffective at collimating outflows. The instability generates internal pressure which helps in decollimating the outflow. Even if the jet starts fully collimated, it is decollimated into a cone of $\sim 45°$ if the toroidal field is the only collimating agent. For flows generated in the magnetic field of an accretion disk, however, the disk field has a strong collimating effect if most of the poloidal magnetic flux (number of field lines crossing the disk plane) is in the outer parts of the disk, as pointed out before (Blandford 1993, Spruit 1994). We have shown how in this collimation mechanism the opening angle of the jet depends on the degree of central concentration of the poloidal flux in the disk and on the ratio of outer to inner disk radii. As an example, a jet from a disk in which this ratio is 10^4 or 10^5 (AGN or protostellar disks, for example), would have opening angles of less than 4 or 1.5 degrees, respectively, if the field strength on the disk varies as r^{-1}. For type II AGN jets with a nominal Lorentz factor of 10 this translates into observed opening angles of 0.4 and 0.15 degrees (since the apparent lateral expansion is reduced due to the transversal Doppler effect). For disks of smaller relative size however, the collimation is much less pronounced. Disks in Cataclysmic Variables, for example, have a radius of the order $3\,10^{10}$ cm, while their inner radius is limited by the radius of the white dwarf, of the order 10^9 cm. For these parameters, we find opening angles of at least $20°$ (see figure 8). This agrees with the observation that no jets are known from these systems, though outflows have been observed in several cases. They are inferred to be relatively uncollimated (Woods et al. 1990, 1992).

These poloidally collimated jets have somewhat different properties from the standard toroidally collimated jets.

Because of the decay of the poloidal field, the Poynting flux (which is carried entirely by the toroidal field) is negligible. The decay of the toroidal field also has the consequence that the flow exceeds the fast magnetosonic speed soon after passing through the Alfvén surface, as opposed to toroidally confined jets where the fast magnetosonic surface can be at very large distances. Since the acceleration of the flow stops at the fast magetosonic surface, the asymptotic flow speed is close to the flow speed at the Alfvén surface. Theeffective 'launching surface' in these jets is thus the Alfvén surface. A new critical distance now plays a role, namely that at which the radial expansion speed of the jet reaches the Alfvén speed. Beyond this distance, the flow can no longer be collimated by the surrounding poloidal field, hence this is the 'distance of last collimation', or *collimation distance* z_c for short. It does not play a role in toroidally collimated flows, in which the radial flow never exceeds the Alfvén speed (with the possible exception of the nearly uncollimated 'conical' flows discussed by Li et al., 1992). Outside the collimation distance, the flow expands ballistically at a constant speed equal to the Alfvén speed at z_c. The opening angle is fixed after this (a narrow 'conical' outflow). The collimation distance can be much larger than the Alfvén distance, but is not much larger than than the size R of the disk. This is typically not resolved observationally (with the exception of VLBI observations of some AGN jets).

The jets computed here have the interesting property of being *magnetically accelerated* and *magnetically collimated*, but yet are practically *nonmagnetic* beyond the collimation distance. Their energy flux is kinetic, and their radial expansion is ballistic (i.e. they are unconfined) beyond this distance.

On the basis of our model we interpret the observed jets as being only the *ballistic end products* of something that happened on a much smaller length scale. No external medium is needed to explain observed narrow opening angles of these jets, and no interaction with an external medium is necessary to explain the parallel field orientation observed in many fast jets (section 4.4). Since the toroidal field has disappeared shortly after the Alfvén surface, it can not play a role in any helical structure seen in jets. Where such structures are seen we infer that they must be due to other causes, most likely a slight precession of the jet, or a binary companion of the jet-producing object (e.g. Hardee et al. 1994, Conway and Wrobel 1995).

The poloidal configurations for the disk field which we have assumed here might be considered somewhat hypothetical. In particular, they would not result naturally from any dynamo process in the disk, which is much more likely to generate a small scale field of mixed polarity (Hawley et al. 1995, Brandenburg et al. 1995). They would result rather naturally, however, by the compression of magnetic flux captured by the disk from its environment. We have argued elsewhere (Spruit Stehle and Papaloizou, 1995) that such fields can reach quite substantial strengths before becoming unstable. Capture would also tend to produce a field in which most of the magnetic flux remains stored in the outer parts of the disk, as required for poloidal collimation. The exact dependence of the field strength on radius in the disk remains conjectural, howvever. We have shown that a dependence $B \sim r^{-\mu}$ with $\mu \lesssim 1.3$ is sufficient, but it remains to be investigated whether the poloidal fields in real accretion disks satisfy these requirements.

ACKNOWLEDGMENTS

The work reported here was done as part of the research network 'accretion onto compact objects and protostars' supported by EC grant ERB–CHRX–CT93–0329. We thank an anonymous referee for constructive criticism.

REFERENCES

Appl S., 1996, A&A submitted
Appl S., Camenzind M., 1993, A&A 270, 71
Appl S., Camenzind M., 1992, A&A 256, 354
Bateman G., 1980, MHD Instabilities, MIT Press, Cambridge, Mass.
Bell A.R., Lucek S.G., 1995, MNRAS 277, 1327
Blandford, R.D., 1993, in D. Burgarella, M. Livio and C. O'Dea, eds., Astrophysical Jets, Cambridge: Cambridge University Press, p.15
Blandford, R.D. and Payne, D.G.: 1982, MNRAS 199, 883
Brandenburg, A., Nordlund, Å., Stein, R.F., Torkelsson, U., 1995, ApJ 446, 741
Cao, X.-W. Spruit H.C. 1994, A&A 287, 80
Choudhuri, A.R., Königl, A., 1986, ApJ 310, 96
Conway J.E., Wrobel J.M., 1995, ApJ 439, 98
Craig I.J.D., Sneyd A.D., 1990, ApJ 357, 653
Eichler, D., 1993, ApJ 419, 111
Fendt C., Camenzind M., Appl S., 1995, A&A 300, 791
Galsgaard K., 1996, J. Geophys. Res., in press
Hardee P.E., Cooper M.A., Clarke D.A., 1994, ApJ 424, 126
Hawley, J.F., Gammie, C.F. and Balbus, S.A., 1995, ApJ 440, 742
Heyvaerts J., Norman C.A., 1989, ApJ 347, 1055
Heyvaerts J. and Norman C.A., 1997, in prepapration
Horiuchi R., Sato T., 1986, Phys. Fluids 29, 1161
Königl A., Choudhuri A.R., 1985, ApJ 289, 173
Königl A., Ruden, S.P.: 1993, in E.H. Levy, J.I. Lunine, eds., Protostars and Planets III, Univerity of Arizona Press, Tucson, p.641
Li Z., Chiueh, T., Begelman, M.C., 1992, ApJ 394, 459
Li Z., 1996, ApJ, in press.
Lucek S.G., Bell A.R., 1996, MNRAS 281, 245
Nitta S.-Y., 1994, PASJ 46, 217
Peter W., Eichler D., 1993, ApJ 417, 170
Peter W., Eichler D., 1995, ApJ 438, 244
Pitts E., Tayler R.J., 1985 MNRAS 216, 139
Sakurai, 1987, PASJ 39, 821
Sauty C., Tsinganos K. 1994, A&A 287, 893
Spruit H.C., 1994, in D. Lynden-Bell, ed., Cosmical Magnetism, Kluwer, Dordrecht, p. 33
Spruit H.C., 1996, in R.A.M.J. Wijers, M.B. Davies, C.A., Tout, eds., Physical Processes in Binary Stars, Kluwer, Dordrecht, p.249
Spruit H.C., Stehle R., Papaloizou, J.C.B., 1995, MNRAS 275, 1223
Stehle R., 1997, in preparation
Tayler R.J., 1980, MNRAS 191, 151
Taylor J.B., 1974, Phys. Rev. Lett. 33, 1139
Todo Y., 1993, in ESA, Fourth International Toki Conference on Plasma Physics and Controlled Nuclear Fusion (Nat. Inst. for Fusion Science, Nagoya), p.337
Tomimatsu A., 1994, PASJ 46, 123
Todo Y., Uchida Y., Sato T., Rosner R., 1993, ApJ 403, 164
Uchida Y., Shibata K., 1984, PASJ 36, 105
Uchida Y., Shibata K., 1985, PASJ 37, 515

Villata M., Ferrari A., 1994, A&A 284, 663
Woltjer L., 1958, Proc. Nat Acad. Sci. 44, 489
Woods J.A., Drew J.E., Verbunt F., 1990, MNRAS 245, 323
Woods J.A., Verbunt F., Cameron A.C., Drew J.E., Piters A., 1992, MNRAS 255, 237

6 APPENDIX

The vector potential $\mathbf{A}_{\rm R}(r,\varphi,z) = A_{\rm R}(r,\varphi,z)\mathbf{e}_\varphi$ follows from the Biot-Savart equation:

$$A_R(r,\varphi,z) = J_0\int_0^R\int_0^{2\pi}\left(\frac{R}{x}\right)^\mu \frac{x{\rm d}x\cos\varphi{\rm d}\varphi}{(x^2+z^2+r^2-2xr\cos\varphi)^{\frac{1}{2}}}. \quad (38)$$

We calculate the magnetic field B_r, B_z near the axis by making an expansion in $x/R \ll 1$ in the integral (38). For this purpose we consider the finite disk as the difference between an infinite disk as studied by Sakurai (1987) and an infinite annulus for $r > R$. The vector potential δA_R created by the annulus extending to infinity outside of the disk of radius R is:

$$A_R = A_\infty - \delta A_R, \qquad \delta A_R = \quad (39)$$

$$J_0\int_R^\infty\int_0^{2\pi}\left(\frac{R}{x}\right)^\mu \frac{\cos\varphi}{(x^2+z^2)^{\frac{1}{2}}}\frac{x{\rm d}x{\rm d}\varphi}{\left(1+\frac{r^2-2xr\cos\varphi}{x^2+z^2}\right)^{\frac{1}{2}}}. \quad (40)$$

The first order is:

$$\delta A_R(r,\varphi,z) = J_0\pi\frac{r}{R}\left(\frac{R}{z}\right)^\mu\int_0^{\frac{z}{R}}\frac{u^{\mu-1}{\rm d}u}{(u^2+1)^{\frac{3}{2}}} + \mathcal{O}\left(\frac{r^3}{R^3}\right). \quad (41)$$

Thus the magnetic field $\delta\mathbf{B} = \nabla\times\delta\mathbf{A}$ produced by the infinite annulus $r > R$ is:

$$\delta B_r = -3\pi J_0\frac{r}{R}\left(\frac{R}{z}\right)^{1+\mu}\int_0^{\frac{z}{R}}\frac{u^{\mu+1}{\rm d}u}{(u^2+1)^{\frac{5}{2}}} + \mathcal{O}\left(\frac{r^3}{R^3}\right), \quad (42)$$

$$\delta B_z = 2\pi J_0\left(\frac{R}{z}\right)^\mu\int_0^{\frac{z}{R}}\frac{u^{\mu-1}{\rm d}u}{(u^2+1)^{\frac{3}{2}}} + \mathcal{O}\left(\frac{r^2}{R^2}\right). \quad (43)$$

The magnetic field created by the infinite disk $\mathbf{B}_\infty = \nabla\times\mathbf{A}_\infty$ was calculated by Sakurai (1987) in terms of the hypergeometric function F:

$$B_r^\infty = \frac{\pi J_0}{K_1}\frac{r}{z}\left(\frac{R}{z}\right)^\mu F(\frac{\mu+1}{2},\frac{\mu+2}{2},2,-\frac{r}{z^2}), \quad (44)$$

$$B_z^\infty = \frac{2\pi J_0}{\mu K_1}\left(\frac{R}{z}\right)^\mu F(\frac{\mu}{2},\frac{\mu+1}{2},1,-\frac{r}{z^2}), \quad (45)$$

where the constant K_1 is defined by

$$K_1 = \frac{2^{\mu-1}\Gamma(\frac{\mu+1}{2})}{\Gamma(1-\frac{\mu-1}{2})\Gamma(\mu+1)}. \quad (46)$$

The first order magnetic field of the finite disk near the axis is the difference $\mathbf{B} = \mathbf{B}_\infty - \delta\mathbf{B}$, and is given by Eqs. (23) and (25).
The variation of the angle θ along a field line close to the axis can be written as follows:

$$\mathbf{B}\cdot\nabla\tan\theta = \frac{rB_z}{R^2}\left(\frac{\partial\Psi}{\partial s}+\Psi^2\right)(s) + \mathcal{O}\left(\frac{r^3}{R^3}\right), \quad (47)$$

$$\Psi(s) = \frac{\mu}{2s}\frac{1+3K_1\int_0^s\frac{u^{\mu+1}{\rm d}u}{(u^2+1)^{\frac{5}{2}}}}{1-\mu K_1\int_0^s\frac{u^{\mu-1}{\rm d}u}{(u^2+1)^{\frac{3}{2}}}}, \quad (48)$$

where $s = z/R$. The height $z_{\rm x} = s_{\rm x}R$ where the angle θ is minimum corresponds to an inflection point of the flow line. The coefficient $s_{\rm x}(\mu)$ is a solution of the following dimensionless equation:

$$\left(\frac{\partial\Psi}{\partial s}+\Psi^2\right)(s_{\rm x}) = 0. \quad (49)$$

In order to estimate the value of the minimum angle $\theta_{\rm min}(r_{\rm i})$ along a field line anchored in the disk at the radius $r_{\rm i} \ll R$, we use the conservation of the magnetic flux $\Phi(r_{\rm i})$ along the flux tube of radius $r_{\rm i}$ in the disk. To calculate this flux we use the expression of the vertical magnetic field in an infinite disk calculated by Sakurai (1987), and correct it for the contribution of the infinite annulus $r > R$:

$$\int_0^{r_{\rm i}} B_z^\infty(r,z=0)r{\rm d}r = \frac{\pi J_0}{\mu K_2}\left(\frac{r_{\rm i}}{R}\right)^{2-\mu}R^2, \quad (50)$$

where

$$K_2 = \frac{2-\mu}{2\mu}\frac{\Gamma(\frac{\mu+1}{2})\Gamma(1-\frac{\mu}{2})}{\Gamma(\frac{\mu}{2})\Gamma(1-\frac{\mu-1}{2})}. \quad (51)$$

According to Eq. (43) for $z \to 0$, the vertical field created by the infinite annulus is regular at the origin, thus the total flux is:

$$\Phi(r_{\rm i}) = \frac{\pi J_0}{\mu K_2}\left(\frac{r_{\rm i}}{R}\right)^{2-\mu}\left[1-K_2\left(\frac{r_{\rm i}}{R}\right)^\mu\right]R^2. \quad (52)$$

The contribution of the infinite annulus to the flux near the axis is therefore important only in the limit of $\mu \to 1$.

The flux at the height z and distance $r \ll R$ is, at first order, $B_z(r=0,z)r^2/2$, so that the distance to the axis, at the height z, of the field line anchored at $r_{\rm i} \ll 1$ is

$$r(r_{\rm i},z) = \left[\frac{2\Phi(r_{\rm i})}{B_z(r=0,z)}\right]^{\frac{1}{2}} = \mathcal{O}\left[\left(\frac{r_{\rm i}}{R}\right)^{1-\frac{\mu}{2}}\left(\frac{R}{z}\right)^{\frac{\mu}{2}}\right]R \ll R. \quad (53)$$

Applying this to the the height of the inflection point, we obtain Eq. (29), with

$$C = \frac{\mu}{(2s_{\rm x})^{1-\frac{\mu}{2}}}\left[\frac{\Gamma(\frac{\mu}{2})}{(2-\mu)\Gamma(1-\frac{\mu}{2})\Gamma(\mu)}\right]^{\frac{1}{2}}\times \frac{1+3K_1\int_0^{s_{\rm x}}\frac{u^{\mu+1}{\rm d}u}{(u^2+1)^{\frac{5}{2}}}}{\left[1-\mu K_1\int_0^{s_{\rm x}}\frac{u^{\mu-1}{\rm d}u}{(u^2+1)^{\frac{3}{2}}}\right]^{\frac{3}{2}}}. \quad (54)$$